Chalcogenide Letters Vol. 15, No. 10, October 2018, p. 475 - 481

EFFECT OF SUBSTRATE SURFACE ON THE GROWTH OF SPRAY DEPOSITED Cu_2ZnSnS_4 THIN FILMS

U. CHALAPATHI, B. POORNAPRAKASH, S. H. PARK*
Department of Electronic Engineering, Yeungnam University, Gyeongsan 38541, South Korea

We report on the growth and properties of Cu_2ZnSnS_4 thin films spray-deposited on soda-lime glass (SLG) and Mo-, SnO_2:F (FTO)-, and ZnO:Al (AZO)- coated glass substrates. The compositional, structural, microstructural, and optical properties of the films were analyzed as a function of substrate surface. The films (prepared under identical conditions) exhibited different grain sizes because of substrate surface difference. Film growth on Mo and FTO surfaces was uniform, but that on SLG was nonuniform, and we observed grain clustering. Grain growth on the AZO surface was very low and nonuniform. The direct optical bang gap of the films was 1.38 eV.

(Received August 13, 2018; Accepted October 4, 2018)

Keywords: Thin films, Cu_2ZnSnS_4, Spray pyrolysis, Absorber, Photovoltaic

1. Introduction

Cu_2ZnSnS_4 (CZTS) has gained much attention in recent years as an absorber in thin film photovoltaics owing to its direct optical band gap of 1.45 eV, high optical absorption coefficient ($\alpha > 10^4$ cm^{-1}), p-type electrical conductivity, and the presence of earth-abundant constituent elements. CZTS-based thin film solar cells exhibit a conversion efficiency of 11% [1] at the laboratory level. Various research groups have focused on the growth of these films using different physical vapor deposition techniques such as sputtering [2, 3], evaporation [4—9], pulsed laser deposition [10] followed by sulfurization, and chemical methods such as spray pyrolysis [11—13], electrodeposition [14—16], sol-gel synthesis [17, 18], successive layer adsorption and reaction [19], etc. Among the chemical methods mentioned, spray pyrolysis is a simple, suitable, and cost-effective technique to obtain good quality films over a large area.

Extensive studies on the preparation of CZTS thin films and devices by spray pyrolysis have been performed by different research groups in the past decade. Nakayama and Ito [11] have reported the growth and properties of CZTS thin films fabricated using spray pyrolysis for the first time in 1996. Madarasz et al. [20] have carried out studies on thermal decomposition of precursors: thiourea complexes of Cu, Zn, and Sn chlorides for spray pyrolysis, and they have studied the effect of substrate temperature from 225 to 350 ^oC. Kamoun et al. [21] have reported the effect of substrate temperature in the range 280—360 ^oC on CZTS film growth. Kishore Kumar et al. [12, 13, 22] have investigated the effects of substrate temperature (290—450 ^oC), solution pH, and Cu salt and thiourea concentrations on the growth of CZTS films. Prabhakar et al. [23, 24] have studied the effects of substrate temperature and incorporation of Na from glass substrates on CZTS film growth. Rajeshmon et al. [25] have studied the role of Sn salt in controlling the optoelectronic properties of spray-deposited CZTS thin films. Yoo et al. [26] studied the comparison between spray and sulfurization and showed that with an additional sulfurization step, improvement in crystallinity of sprayed CZTS films to the level of the sulfurized metallic films. Das et al. [27] have investigated effects of substrate temperature and molarity of precursors on CZTS film growth. Patel et al. [28, 29] have used the spray technique to deposit CZTS films under a non-equilibrium condition without the sulfurization step. In addition, they have fabricated a CZTS-based solar cell [29]. Huang et al. [30] have prepared CZTS films by ultrasonic spray pyrolysis and studied the

* Corresponding author: sihyun_park@ynu.ac.kr

effect of substrate temperature on the structural, morphological, and photo-electrochemical properties of CZTS films. Seboui et al. [31] have investigated the effect of substrate temperature on CZTS film growth. Gurieva et al. [33] have studied the effect of addition of a small quantity of C_2H_5OH to the precursor solution during CZTS film growth. Rodriguez et al. [33] have investigated the influence of precursor solution concentration and annealing conditions on CZTS film growth.

Growth of CZTS thin films on transparent conducting oxide coated glass substrates is essential for achieving high efficiency tandem and bifacial solar cells [34]. Nakada et al. [9] have prepared Cu(In,Ga)Se_2 (CIGS) thin films on SnO_2:F (FTO)-coated glass substrates. They have also fabricated semitransparent CIGS thin film solar cells for top tandem and bifacial devices with FTO as a back contact. They have reported that CIGS solar cells fabricated on FTO substrates below 520 ^oC exhibit efficiency equal to that of cells fabricated onto Mo substrates. An interaction between the film and the substrate can cause a strain in the deposited films, which alters the device efficiency. Thus, it is very essential to control the of film formation on the substrate surface. In the present investigation, we have performed a comparative study of the growth of CZTS thin films deposited on different substrate surfaces by a simple and an inexpensive spray pyrolysis technique. For the deposition, we have used the following substrates: soda-lime glass (SLG), Mo-, SnO_2:F (FTO)-, and ZnO:Al (AZO)-coated glass. The results are presented in Section 3.

2. Experimental details

We prepared the starting solutions for the growth of CZTS thin films by dissolving Analar grade cupric chloride (0.01 M), zinc acetate (0.005 M), stannic chloride (0.005 M), and thiourea (0.04 M) in distilled water. The solutions were sprayed onto SLG-, and Mo-, FTO-, and AZO-coated glass substrates using a spray nozzle. The substrate temperature was maintained at 400 ^oC. The solution flow rate was maintained at 15 mL/min. The as-prepared thin films were annealed in a two-zone tubular furnace at 550 ^oC in for 1 h under 1 mbar ($N_2 + S_2$) pressure.

X-ray diffraction (XRD) patterns of the films were recorded on a Bruker D8 Advanced diffractometer in the 2θ range 10-60^0 with Cu Kα radiation (λ = 0.15406 nm). Raman spectra were collected on a Horiba Jobin Yvon HR 800UV confocal micro-Raman spectrometer in the backscattering mode using a Nd:YAG laser source (λ = 532 nm) and a grating with 1800 lines/mm. Surface morphology and elemental composition were studied by scanning electron microscopy (SEM; Carl Zeiss, ULTRA-55) and energy dispersive※ray spectrometry (EDS; Oxford Instruments, U.K). Transmittance curves of the films were obtained on a Perkin Elmer ultraviolet-visible-near infrared (UV-Vis-NIR) double beam spectrophotometer (LAMDA 950).

3. Results and discussion

3.1. Composition

Table 1 shows the elemental composition data of CZTS films deposited onto different substrate surfaces. The composition of these films is mostly non-stoichiometric CZTS. The films grown onto SLG and Mo-coated substrates are slightly Zn-poor and those grown onto FTO-coated glass substrates are Sn-rich and slightly Cu-poor.

Table 1. Elemental composition data of CZTS films grown on different substrate surfaces.

S.No	Substrate surface	Atomic percent				Ratio		
		Cu	Zn	Sn	S	Cu/(Zn+Sn)	Zn/Sn	S/M
1	SLG	23.5	11.2	13.3	52.0	0.96	0.84	1.08
2	Mo	22.4	11.3	13.1	53.1	0.92	0.86	1.13
3	FTO	20.7	10.6	15.7	53.0	0.79	0.67	1.13
4	AZO	19.1	16.7	12.0	52.3	0.67	1.39	1.10

The films grown onto AZO-coated substrates are Zn-rich and Cu-poor. The films grown onto FTO-coated substrates are Sn-rich because the presence of Sn in the substrate itself and those grown AZO-coated substrates are Zn-rich because of the presence of Zn on the substrate surface.

3.2. Structural analysis

Fig. 1 shows the XRD patterns of CZTS films deposited onto SLG, Mo, FTO and AZO surfaces, exhibiting an intense peak at (112) followed by weak peaks at (101), (200), (220) and (312) correspond to CZTS (JCPDS Card No. 26-0575). The slight difference in the intense peak positions may be due to the strain induced in the films during deposition/annealing.

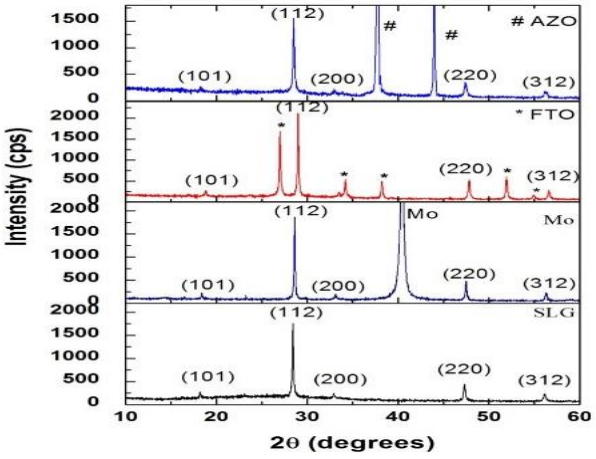

Fig. 1 XRD patterns of CZTS films grown on different substrate surfaces.

The strain in the films can be attributed to the difference in the thermal expansion coefficients of the substrates and the films. The films exhibit a preferential orientation along (112) plane. We have estimated the crystallite size (D), strain (ε), and dislocation density (δ) using the following formulae [35]:

$$D = k\lambda/\beta \cos\theta \quad (1)$$

where k is a shape factor and β is full width at half maximum (FWHM).

$$\varepsilon = \beta \cos\theta/4 \quad (2)$$

$$\text{and } \delta = 1/D^2 \quad (3)$$

Table 2 lists the estimated lattice parameter, crystallite size, strain, and dislocation density values of the films grown onto different substrate surfaces. A slight variation in the lattice parameters, as seen, is attributed to an induced strain in the films.

The crystallite sizes gradually decrease from 60 nm to 47 nm for films deposited onto SLG, Mo, FTO, and AZO surfaces, respectively. The relatively large crystallite size observed for films deposited on SLG is possible due to the Na ion diffused from the substrate to the film [24]. In the case of films grown on the other surfaces, the respective Mo, FTO, and AZO layers present in between the glass substrate and the CZTS film may inhibit the diffusion of Na ions from glass to the film, resulting in the formation of smaller crystallites. The strain and dislocation density of CZTS films are found to increase (Table 2) on depositing from SLG to AZO surfaces.

Table 2. Lattice parameter, crystallite size, strain, and dislocation density values of CZTS films grown on different substrate surfaces.

Substrate surface	Lattice parameters		Crystallite size (nm)	Strain	Dislocation density (nm^{-2})
	a (nm)	c (nm)			
SLG	0.542	1.091	60	$0.59x10^{-3}$	$0.27x10^{-3}$
Mo	0.541	1.078	55	$0.67x10^{-3}$	$0.33x10^{-3}$
FTO	0.537	1.105	50	$0.71x10^{-3}$	$0.40x10^{-3}$
AZO	0.541	1.084	47	$0.75x10^{-3}$	$0.45x10^{-3}$

We have used Raman spectroscopy as a complementary tool to detect the possible phases in the films. Micro-Raman spectra of CZTS films grown onto different substrate surfaces are shown in Fig. 2. Raman spectra of the films deposited onto SLG exhibit an intense mode at 336 cm^{-1} and two weak modes at 286 cm^{-1} and 366 cm^{-1}. All the observed modes closely match with those reported Raman modes for CZTS [36—39]. Raman spectra of the films deposited onto Mo and FTO surfaces exhibit an intense mode at 335 cm^{-1} and two weak modes at 286 cm^{-1} and 366 cm^{-1}. An additional mode that is observed at 410 cm^{-1} for the films deposited onto the Mo-coated substrate is due to MoS_2 phase. The intense mode position further shifts to 334 cm^{-1} for films grown onto AZO-coated glass substrates. The slight shift in the intense Raman mode position with respect to the substrate surface is possibly due to the induced strain [26] and/or disorder in the cation sub lattices [40] in the films. There is a slight increase in the FWHM of the intense Raman modes of CZTS films grown onto SLG to AZO surfaces indicating the decrease in the crystallinity as confirmed by XRD analysis.

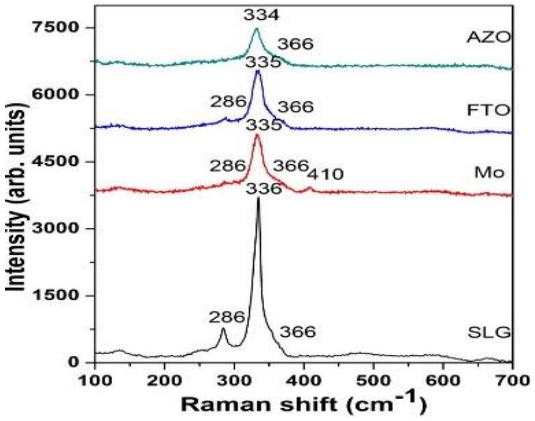

Fig. 2. Raman spectra of CZTS films deposited on different substrates.

3.3. Microstructure

Fig. 3 shows the SEM images of CZTS films grown onto different substrate surfaces. The micrograph of the film deposited onto the SLG substrate shows distinct grains with bright and dark contrasts. The bright grains are due to Sn-rich CZTS and the dark grains are due to Sn-correct CZTS. Therefore, the morphology of the films grown onto the SLG surface is nonuniform. The average grain size is found to be 1.5 μm.

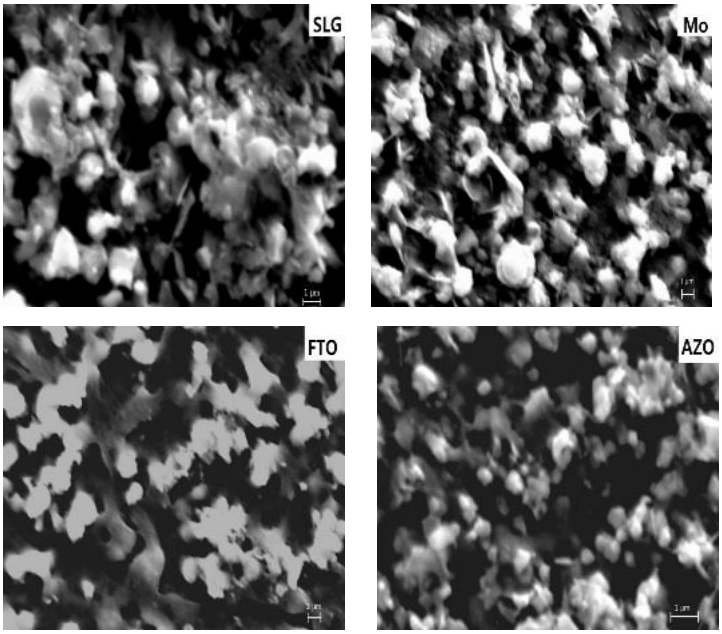

Fig. 3 SEM images of CZTS films grown on different substrate surfaces.

The nonuniform grain growth is possibly due to the amorphous nature of SLG. In addition, the observed large grains may be due to the Na ions that diffused from SLG to the film [24]. The films grown on Mo-coated surfaces exhibit uniform morphology with an average grain size of 1 μm. The films grown onto the FTO-coated glass substrates also exhibit uniform morphology with 2 μm grains; the formation of the large grains is attributed to the removal of fluorine by diffusion at the CZTS/FTO interface during high-temperature deposition [41]. The morphology of films grown onto AZO surfaces is nonuniform and the average grain size is less than 1 μm. Thus, the films grown onto different substrate surfaces exhibit different grain sizes, indicating that the growth of the CZTS film dependent on the type of substrate surface.

3.4. Optical absorption

Fig. 4(a) shows the spectral transmittance curves of CZTS films deposited onto SLG, FTO, and AZO surfaces. The curves of films deposited onto Mo-coated glass substrates were not recorded because of the opaque nature of the Mo layer. The fundamental absorption edge of the films deposited onto the other three surfaces starts at 870 nm and ends at 750 nm. The low transmittance of the films possibly due to the diffuse nature of the films.

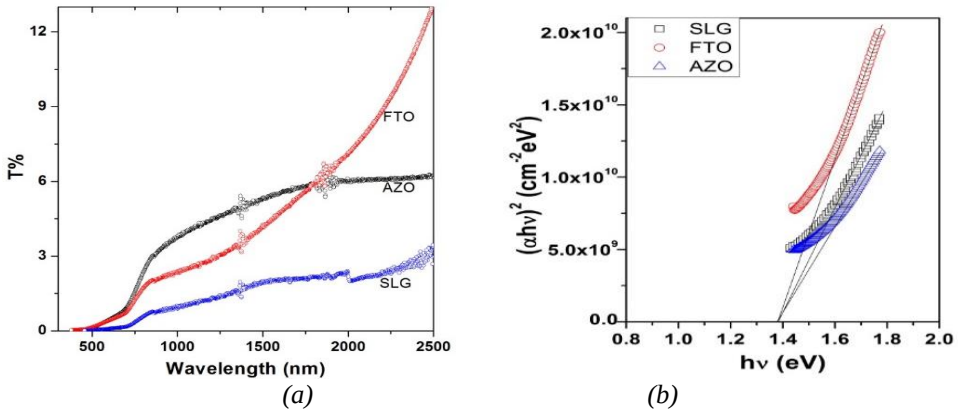

Fig. 4. (a) Optical transmittance curves and (b) $(\alpha h\nu)^2$ versus hν plots of CZTS films grown on different substrate surfaces.

Fig. 4(b) shows the $(\alpha h\nu)^2$ versus $h\nu$ plots of CZTS films grown onto SLG, FTO and AZO surfaces. The direct optical band gap of the films, determined from the data is 1.38 eV; the value reported in the literature is in the range 1.45--1.60 eV [2, 5]. The band gap values determined in this study is slightly lower than the reported values because of slight variations in film composition/crystallinity.

4. Conclusions

Cu_2ZnSnS_4 (CZTS) thin films were grown on different substrate surfaces by spray pyrolysis. The films exhibited kesterite structure with preferred orientation along the (112) plane. The films grown onto Mo- and FTO-coated glass substrates were uniform with large grains (> 1 μm); however, the films deposited onto SLG substrates were nonuniform, and grain clustering was observed. The grain growth was very low and nonuniform in the case of films deposited onto AZO surfaces. The direct optical band gap of the films was determined to be 1.38 eV.

Acknowledgement

This work was supported by the National Research Foundation of Korea (NRF) grant funded by the Korea government (MOE) (No. NRF-2017R1D1A3B03034243) and by the Technology Innovation Program (10067492) funded by the Ministry of Trade, Industry & Energy (MOTIE, Korea).

References

[1] C. Yan, J. Huang, K. Sun, S. Johnston, Y. Zhang, H. Sun, A. Pu, M. He, F. Liu, K. Eder, L. Yang, J. M. Cairney, N. Ekins-Daukes, Z. Hameiri, J. A. Stride, S. Chen, M. Green, X. Hao, Nat. Energy doi.org/10.1038/s41560-018-0206-0, 1 (2018).
[2] K. Ito, T. Nakazawa, Jpn. J. Appl. Phys. **27**, 2094 (1988).
[3] K. Jimbo, R. Kimura, T. Kamimura, S. Yamada, W. S. Maw, H. Araki, K. Oishi, H. Katagiri, Thin Solid Films **515**, 5997 (2007).
[4] T. M. Friedlmeier, H. Dittrich, H.-W. Schock, Institute of Physics Conference Series **152**, Bristol, England, Boston: Adam Hilger, Ltd., 345 (1985).
[5] H. Katagiri, K. Saitoh, T. Washio, H. Shinohara, T. Kurumadani, S. Miyajima, Sol. Energy Mater. Sol. Cells **65**, 141 (2001).
[6] H. Katagiri, K. Jimbo, K. Moriya, K. Tsuchida, Photovoltaic Energy Conversion, Proceedings of 3rd World Conference on IEEE **3**, 2874 (2003).
[7] T. Kobayashi, K. Jimbo, K. Tsuchida, S. Shinoda, T. Oyanagi, H. Katagiri, Jpn. J. Appl. Phys. **44**, 783 (2005).
[8] H. Araki, A. Mikaduki, Y. Kubo, T. Sato, K. Jimbo, W. S. Maw, H. Katagiri, M. Yamazaki, K. Oishi, A. Takeuchi, Thin Solid Films **517**, 1457 (2008).
[9] U. Chalapathi, S. Uthanna, V. Sundara Raja, J. Renew. Sustain. Energy **5**, 031610 (2013).
[10] K. Moriya, K. Tanaka, H. Uchiki, Jpn. J. Appl. Phys. **47**, 602 (2008).
[11] N. Nakayama, K. Ito, Appl. Surf. Sci. **92**, 171 (1996).
[12] Y. B. Kishore Kumar, G. Suresh Babu, P. Uday Bhaskar, V. Sundara Raja, Sol. Energy Mater. Sol. Cells **93**, 1230 (2009).
[13] Y. B. Kishore Kumar, G. Suresh Babu, P. Uday Bhaskar, V. Sundara Raja, Phys. Stat. Sol.A **206**, 1525 (2009).
[14] J. J. Scragg, P. J. Dale, L. M. Peter, G. Zoppi, I. Forbes, Phys. Stat. Sol. (b) **245**, 1772 (2008).
[15] J. J. Scragg, P. J. Dale, L. M. Peter, Thin Solid Films **517**, 2481 (2009).
[16] R. Schurr, A. Holzing, S. Jost, R. Hock, T. Vif, J. Schulze, A. Kirbs, A. Ennaoui,

M. Lux-Steiner, A. Weber et al., Thin Solid Films **517**, 2465 (2009).
[17] K. Tanaka, N. Moritake, H. Uchiki, Sol. Energy Mater. Sol. Cells **91**, 1199 (2007).
[18] K. Tanaka, N. Moritake, M. Oonuki, H. Uchiki, Jpn. J. Appl. Phys. **47**, 598 (2008).
[19] Z. Su, C. Yan, K. Sun, Z. Han, F. Liu, J. Liu, Y. Lai, J. Li, Y. Liu, Appl. Surf. Science (2012).
[20] J. Madarasz, P. Bombicz, M. Okuya, S. Kaneko, Sol. State Ion. **141**, 439 (2001).
[21] N. Kamoun, H. Bouzouita, B. Rezig, Thin Solid Films **515**, 5949 (2007).
[22] Y. Kumar, P. U. Bhaskar, G. S. Babu, V. S. Raja, Phys. Stat. sol. A **207**, 149 (2010).
[23] T. Prabhakar, J. Nagaraju, 35th IEEE, IEEE, 001964 (2010).
[24] T. Prabhakar, N. Jampana, Sol. Energy Mater. Sol. Cells **95**, 1001 (2011).
[25] V. Rajeshmon, C. S. Kartha, K. Vijayakumar, C. Sanjeeviraja, T. Abe, Y. Kashiwaba, Sol. Energy **85**, 249 (2011).
[26] H. Yoo, J. Kim, Sol. Energy Mater. Sol. Cells **95**, 239 (2011).
[27] S. Das, C. Frye, P. G. Muzykov, K. C. Mandal, ECS Trans. **45**, 153 (2012).
[28] M. Patel, I. Mukhopadhyay, A. Ray, J. Phys. D: Appl. Phys. **45**, 445103 (2012).
[29] M. Patel, I. Mukhopadhyay, A. Ray, Semicon. Sci. Tech. **28**, 055001 (2013).
[30] S. Huang, W. Luo, Z. Zou, J. Phys. D: Appl. Phys. **46**, 235108 (2013).
[31] Z. Seboui, Y. Cuminal, N. Kamoun-Turki, J. Renew Sust. Energy **5**, 023113 (2013).
[32] G. Gurieva, M. Guc, L. Bruk, V. Izquierdo-Roca, A. Perez Rodriguez, S. Schorr, E. Arushanov, Phys. Stat. Sol. C **10**, 1082 (2013).
[33] M. Espindola-Rodriguez, M. Placidi, O. Vigil-Gal_an, V. Izquierdo-Roca, X. Fontane, A. Fairbrother, D. Sylla, E. Saucedo, Thin solid films **535**, 67 (2013).
[34] P. K. Sarswat, M. Snure, M. L. Free, A. Tiwari, Thin Solid Films **520**, 1694 (2012).
[35] G. Williamson, R. Smallman, Iii. Philos. Mag. **1**, 34 (1956).
[36] M. Himmrich, H. Haeuseler, Spectrochim. Acta A Mol. Spec. **47**, 933 (1991).
[37] A.-J. Cheng, M. Manno, A. Khare, C. Leighton, S. Campbell, E. Aydil, J. Vac. Sci. Technol. A **29**, 051203 (2011).
[38] X. Fontane, V. Izquierdo-Roca, E. Saucedo, S. Schorr, V. Yukhymchuk, M. Y. Valakh, A. Perez-Rodriguez, J. R. Morante, J. Alloys Compd. **539**, 190 (2012).
[39] D. Dumcenco, Y.-S. Huang, Opt. Mater. **35**, 419 (2012).
[40] R. Caballero, E. Garcia-Llamas, J. Merino, M. Le_on, I. Babichuk, V. Dzhagan, V. Strelchuk, M. Valakh, Acta Mater. **65**, 412 (2014).
[42] T. Nakada, Thin Solid Films **480**, 419 (2005).